AFRL-RV-PS-TR-2017-0139

AFRL-RV-PS-TR-2017-0139

EFFICIENT NUMERICAL METHODS FOR NONEQUILIBRIUM RE-ENTRY FLOWS

Graham V. Candler

University of Minnesota
110 Union Street SE
Minneapolis, MN 55455

14 January 2014

Final Report

AIR FORCE RESEARCH LABORATORY
Space Vehicles Directorate
3550 Aberdeen Ave SE
AIR FORCE MATERIEL COMMAND
KIRTLAND AIR FORCE BASE, NM 87117-5776

DTIC COPY

NOTICE AND SIGNATURE PAGE

Using Government drawings, specifications, or other data included in this document for any purpose other than Government procurement does not in any way obligate the U.S. Government. The fact that the Government formulated or supplied the drawings, specifications, or other data does not license the holder or any other person or corporation; or convey any rights or permission to manufacture, use, or sell any patented invention that may relate to them.

This report is the result of contracted fundamental research which is exempt from public affairs security and policy review in accordance with AFI 61-201, paragraph 2.3.5.1. This report is available to the general public, including foreign nationals. Copies may be obtained from the Defense Technical Information Center (DTIC) (http://www.dtic.mil).

AFRL-RV-PS-TR-2017-0139 HAS BEEN REVIEWED AND IS APPROVED FOR PUBLICATION IN ACCORDANCE WITH ASSIGNED DISTRIBUTION STATEMENT.

//SIGNED//	//SIGNED//
Dr. Raymond Bemish	Dr. Thomas R. Caudill, Acting Chief
Program Manager, AFRL/RVBYE	AFRL Battlespace Environment Division

This report is published in the interest of scientific and technical information exchange, and its publication does not constitute the Government's approval or disapproval of its ideas or findings.

REPORT DOCUMENTATION PAGE

Form Approved
OMB No. 0704-0188

1. REPORT DATE *(DD-MM-YYYY)*	**2. REPORT TYPE**	**3. DATES COVERED** *(From - To)*
14-01-2014	Final Report	29 Nov 2011 – 31 Oct 2012

4. TITLE AND SUBTITLE
Efficient Numerical Methods for Nonequilibrium Re-Entry Flows

5a. CONTRACT NUMBER
FA9453-12-1-0133

5b. GRANT NUMBER

5c. PROGRAM ELEMENT NUMBER
62601F

6. AUTHOR(S)
Graham V. Candler

5d. PROJECT NUMBER
1010

5e. TASK NUMBER
PPM00035340

5f. WORK UNIT NUMBER
EF129268

7. PERFORMING ORGANIZATION NAME(S) AND ADDRESS(ES)
University of Minnesota
110 Union Street SE
Minneapolis, MN 55455

8. PERFORMING ORGANIZATION REPORT NUMBER

9. SPONSORING / MONITORING AGENCY NAME(S) AND ADDRESS(ES)
Air Force Research Laboratory
Space Vehicles Directorate
3550 Aberdeen Avenue SE
Kirtland AFB, NM 87117-5776

10. SPONSOR/MONITOR'S ACRONYM(S)
AFRL/RVBYE

11. SPONSOR/MONITOR'S REPORT NUMBER(S)
AFRL-RV-PS-TR-2017-0139

12. DISTRIBUTION / AVAILABILITY STATEMENT

Approved for public release; distribution is unlimited.

13. SUPPLEMENTARY NOTES

14. ABSTRACT

We propose a new implicit computational fluid dynamics method for steady-state compressible reacting flows. The concept is to decouple the total mass, momentum, and energy conservation equations from the species mass and internal energy equations, and to solve the two equation sets sequentially. With certain approximations to the implicit system, it is possible to dramatically reduce the cost of the solution with little to no penalty on convergence properties. Importantly, the cost of the decoupled implicit problem scales linearly with the number of species, as opposed to the quadratic scaling for the conventional fully-coupled method. Furthermore, the new approach reduces the memory requirements by a significant factor. The decoupled implicit method shows promise for application to aerothermodynamics problems and reacting flows.

15. SUBJECT TERMS
Atmospheric re-entry, hypersonic flow, computational fluid dynamics

16. SECURITY CLASSIFICATION OF:			**17. LIMITATION OF ABSTRACT**	**18. NUMBER OF PAGES**	**19a. NAME OF RESPONSIBLE PERSON**
a. REPORT	**b. ABSTRACT**	**c. THIS PAGE**			**19b. TELEPHONE NUMBER** *(include area code)*
Unclassified	Unclassified	Unclassified	Unlimited	40	Dr. Raymond Bemish

This page is intentionally left blank.

TABLE OF CONTENTS

Technical Accomplishments 1

Decoupled Implicit Method 1

Overlay Method for Trace Chemical Species 4

References 5

Appendix: A Decoupled Implicit Method for Aerothermodynamics and Reacting Flows 6

This page is intentionally left blank.

Technical Accomplishments

We developed an improved numerical method for the simulation of re-entry vehicle flow fields, including finite-rate internal energy relaxation and chemical reactions. This method is applicable to the hard-body flow field, as well as to the vehicle wake. The method and approach are documented in two conference papers and a journal article (attached) [1,2]. The computer code that implements the method was transitioned to AFRL Space Vehicles Directorate for the simulation of re-entry vehicle flow fields.

Prior to the present work, existing numerical simulation approaches used computational fluid dynamics (CFD) methods that were designed for chemical kinetics models involving a fairly small number of chemical species – typically about 10 or less. However, realistic re-entry vehicle flows may involve a much larger number of species due to ablation products, trace species that may be relevant for signatures, and ionization of these species. This can result in perhaps 50 chemical species being important for certain types of analyses. The computational and memory costs of present methods scale with the square of the number of chemical species. This scaling makes the simulation of large chemical kinetics models extremely onerous and limits the analyst's use of more detailed kinetics models.

We have developed a new computational method that reduces the simulation costs using a novel approach. The idea is to decouple the chemical species mass conservation equations from the flow field total mass, momentum, and energy conservation equations. This significantly reduces the cost of simulations because the resulting linear system of equations is simpler to solve. However, there are several issues involving robustness and solution accuracy that had to be resolved. In the following, we give a brief description of the approach; full details are available in the attached manuscript that was published as an *AIAA Journal* article.

Decoupled Implicit Method

The usual approach to the numerical solution of thermo-chemical nonequilibrium flows is to solve the fully-coupled species mass, momentum and energy equations using an implicit time integration method. The cost of this approach scales quadratically with the number of equations being solved. Thus, as the number of chemical species increases, the computational cost drastically increases. We have developed an approach that decouples the species mass and internal energy conservation equations from the total mass, momentum and energy equations. Such an approach is commonly used in the combustion literature; however, we have found that those methods may yield different results from the fully-coupled approach. The following outlines the new decoupled method.

Consider the one-dimensional Euler equations of a thermo-chemical nonequilibrium gas:

$$\frac{\partial U}{\partial t} + \nabla \cdot F = W$$

with:

$$U = \begin{pmatrix} \rho_1 \\ \vdots \\ \rho_{ns} \\ \rho u \\ E_v \\ E \end{pmatrix} \qquad F = \begin{pmatrix} \rho_1 u \\ \vdots \\ \rho_{ns} u \\ \rho u^2 + p \\ E_v u \\ (E+p)u \end{pmatrix} \qquad W = \begin{pmatrix} w_1 \\ \vdots \\ w_{ns} \\ 0 \\ w_v \\ 0 \end{pmatrix}$$

Here, we have neglected the viscous fluxes (mass diffusion, shear stresses, and thermal conduction) for simplicity in the following derivation. The computational methods include all of these terms in the solution of the governing equations. Conventional fully-coupled numerical methods solve the above set of equations. However, consider splitting this equation into two components:

$$\frac{\partial \tilde{U}}{\partial t} + \nabla \cdot \tilde{F} = 0$$

$$\frac{\partial \hat{U}}{\partial t} + \nabla \cdot \hat{F} = \hat{W}$$

With:

$$\tilde{U} = \begin{pmatrix} \rho \\ \rho u \\ E \end{pmatrix} \qquad \tilde{F} = \begin{pmatrix} \rho u \\ \rho u^2 + p \\ (E+p)u \end{pmatrix} \qquad \tilde{W} = \begin{pmatrix} 0 \\ 0 \\ 0 \end{pmatrix}$$

and:

$$\hat{U} = \begin{pmatrix} \rho_1 \\ \vdots \\ \rho_{ns} \\ E_v \end{pmatrix} \qquad \hat{F} = \begin{pmatrix} \rho_1 u \\ \vdots \\ \rho_{ns} u \\ E_v u \end{pmatrix} \qquad \hat{W} = \begin{pmatrix} w_1 \\ \vdots \\ w_{ns} \\ w_v \end{pmatrix}$$

Note that:

$$\hat{F} = u\hat{U}$$

The two equations are mathematically equivalent to the original conservation law.

In discrete finite-volume form, these equations may be written as:

$$\frac{\partial \tilde{U}}{\partial t} + \frac{1}{V}\sum_{\mathrm{f}} \tilde{\mathcal{F}} = 0, \qquad \tilde{\mathcal{F}} = \tilde{F} \cdot \vec{S}$$

$$\frac{\partial \hat{U}}{\partial t} + \frac{1}{V}\sum_{\mathrm{f}} \hat{\mathcal{F}} = \hat{W}, \qquad \hat{\mathcal{F}} = \hat{F} \cdot \vec{S}$$

with the sum over the faces of the finite-volume element. There are many possible ways to solve these two equations. Consider a first-order in time implicit method in which we linearize the flux vectors using:

$$\begin{pmatrix} \tilde{\mathcal{F}} \\ \hat{\mathcal{F}} \end{pmatrix}^{n+1} = \begin{pmatrix} \tilde{\mathcal{F}} \\ \hat{\mathcal{F}} \end{pmatrix}^{n} + \begin{pmatrix} \frac{\partial \tilde{\mathcal{F}}}{\partial \tilde{U}} & \frac{\partial \tilde{\mathcal{F}}}{\partial \hat{U}} \\ \frac{\partial \hat{\mathcal{F}}}{\partial \tilde{U}} & \frac{\partial \hat{\mathcal{F}}}{\partial \hat{U}} \end{pmatrix}^{n} \begin{pmatrix} \delta \tilde{U} \\ \delta \hat{U} \end{pmatrix}^{n}$$

$$\hat{W}^{n+1} = \hat{W}^n + \frac{\partial \hat{W}}{\partial \tilde{U}} \delta \tilde{U}^n + \frac{\partial \hat{W}}{\partial \hat{U}} \delta \hat{U}^n$$

Consider solving these equations in two steps. One such approach would be to first solve for the total mass, momentum and energy, neglecting the term due to the linearization of $\tilde{\mathcal{F}}$ with respect to $\tilde{U}$. Then we have the implicit problem:

$$\frac{V}{\Delta t} \delta \tilde{U}^n + \sum_{\mathrm{f}} \frac{\partial \tilde{\mathcal{F}}}{\partial \tilde{U}} \delta \tilde{U} = -\sum_{\mathrm{f}} \tilde{\mathcal{F}}^n$$

The solution of this linear system provides the velocity field at the future time level, *n*+1. Now, using the fact that $\hat{F} = u\hat{U}$ we can write

$$\hat{\mathcal{F}}^{n+1} = u^{n+1} \hat{U}^n \cdot \vec{S} + u^{n+1} \delta \hat{U}^n \cdot \vec{S}$$

Then the second part of the flux may be obtained by solving the system of equations:

$$\frac{V}{\Delta t} \delta \tilde{U}^n + \sum_{\mathrm{f}} u^{n+1} \delta \hat{U}^n \cdot \vec{S} - V \frac{\partial \hat{W}}{\partial \hat{U}} \delta \hat{U}^n = -\sum_{\mathrm{f}} u^{n+1} \hat{U}^n \cdot \vec{S} + V \hat{W}^n + V \frac{\partial \hat{W}}{\partial \tilde{U}} \delta \tilde{U}^n$$

A first glance, this does not seem to be a substantial improvement over the fully-coupled solution. However, there are some features of this approach that are quite interesting.

First, note that the cost of solving the fully-coupled set of equations varies with the number of equations squared. In this case, that would be $(ns + 5)^2$ for a three-dimensional problem with *ns* chemical species and one internal energy equation. The solution is typically done with the Data-Parallel Line-Relaxation (DPLR) method, involving the iterative solution of a block tridiagonal system of equations [3].

For the decoupled method, the same DPLR method must be applied to the total mass momentum and energy conservation equations. This also has a cost that scales quadratically; in this case a three-dimensional problem would scale as 5^2. The second part of the problem is considerably easier to solve. The flux linearization is simple and as a result, the block tridiagonal problem is reduced in complexity and cost. Since the Jacobian matrix of the source vector is full, the cost of this problem will scale like $(ns + 1)^2$, but with a substantially smaller constant of proportionality than the full DPLR solution. Furthermore, the simplicity of the implicit problem requires less memory than the fully-coupled method. Each neighboring element requires the storage of a Jacobian matrix of size (*ns* + 5) x (ns + 5) for the DPLR method; for hexahedral elements, this is six Jacobian matrices as well as the diagonal. Here, we require the storage of the corresponding 5 x 5 matrices plus a single (*ns* + 1) x (*ns* + 1) matrix. The extension to viscous flows is straight-forward and does not increase the cost of the approach.

There are several technical details that are beyond the scope of the present report (and involve cumbersome nomenclature). We implemented the decoupled method within US3D [4,5], and have found that it converges to a steady-state at approximately the same rate as the fully-coupled method run with the DPLR method in the US3D

computational fluid dynamics code. For a large number of chemical species, the cost per time step is reduced by a factor of about 4.8. The memory savings are also large (about a factor of 5) because only a single large Jacobian matrix must be stored, instead of the usual seven matrices for the fully coupled approach. Details of the cost reduction are presented in the attached paper.

The decoupled approach significantly reduces the computational and memory costs of simulations with large numbers of chemical species. For example, it drastically reduces the cost of computing flows with large numbers of ablation products, or high-enthalpy flows with many ionized species. In the future, there are many possible variants to this approach that could be explored that could further reduce computational costs or allow the approach to be extended to time-accurate implicit simulations.

Overlay Method for Trace Chemical Species

In the original proposal, we planned to implement an overlay approach for flows with trace chemical species. The overlay approach is not general, and only applies to trace species that do not affect the bulk properties of the flow (overall density, vibrational temperature, and temperature, in particular). Because of the success of the new decoupled method, this work was not necessary; it is now far better to simply add additional species to the full flow field calculation, rather than running separate approximate simulations to account for the trace species flow.

References

[1] Candler, G.V., P.K. Subbareddy, and I. Nompelis, "Decoupled Implicit Method for Aerothermodynamics and Reacting Flows," *AIAA Journal*, Vol. 51, No. 5, pp. 1245-1254, May 2013. Also AIAA Paper 2012-5917, Sept. 2012.

[2] Candler, G.V., P.K. Subbareddy, and I. Nompelis, "Analysis of a Decoupled Implicit Method for Aerothermodynamics and Reacting Flows," AIAA Paper 2013-0630, Jan. 2013.

[3] Wright, M.J., D. Bose, and G.V. Candler, "A Data-Parallel Line Relaxation Method for the Navier-Stokes Equations," *AIAA Journal*, Vol. 36, No. 9, pp. 1603-1609, Sept. 1998.

[4] Nompelis, I., T.W. Drayna, and G.V. Candler, "Development of a Hybrid Unstructured Implicit Solver for the Simulation of Reacting Flows Over Complex Geometries," AIAA-2004-2227, June 2004.

[5] Nompelis, I., T.W. Drayna, and G.V. Candler, "A Parallel Unstructured Implicit Solver for Hypersonic Reacting Flow Simulation," AIAA-2005-4867, June 2005.

APPENDIX

A Decoupled Implicit Method for Aerothermodynamics and Reacting Flows

Graham V. Candler*
Pramod K. Subbareddy**
Ioannis Nompelis†
Department of Aerospace Engineering and Mechanics
University of Minnesota
110 Union Street SE
Minneapolis, MN 55455

Abstract

We propose a new implicit computational fluid dynamics method for steady-state compressible reacting flows. The concept is to decouple the total mass, momentum, and energy conservation equations from the species mass and internal energy equations, and to solve the two equation sets sequentially. With certain approximations to the implicit system, it is possible to dramatically reduce the cost of the solution with little to no penalty on convergence properties. Importantly, the cost of the decoupled implicit problem scales linearly with the number of species, as opposed to the quadratic scaling for the conventional fully-coupled method. Furthermore, the new approach reduces the memory requirements by a significant factor. The decoupled implicit method shows promise for application to aerothermodynamics problems and reacting flows.

Nomenclature

A	convective flux vector Jacobian matrix
a	speed of sound (m/s)
C	source vector Jacobian matrix
c_s	species s mass fraction
c_{vs}	translational-rotational specific heat of species s (J/kg K)
E	total energy per volume (J/m^3)
E_v	vibrational energy per volume (J/m^3)
e_v	vibrational energy per mass (J/kg)
$\vec{F}$	convective flux vector
F'	convective flux vector normal to element face
F_v	diffusive flux vector
f	value at element face
h_s°	heat of formation per unit mass (J/kg)
i, j	grid index
k	relaxation step index
L, R	values obtained from left and right data

* Russell J. Penrose and McKnight Presidential Professor, Fellow AIAA
** Post-Doctoral Researcher, Member AIAA
† Research Associate, Member AIAA

ℓ	element on solution line
M, N	Jacobian matrices for linearization of viscous flux
M_s	molar mass of species s (kg/kmol)
n	time step
ns	number of chemical species
p	pressure (Pa)
$\hat{R}$	universal gas constant (J/kmol K)
$\vec{S}, S$	element face area vector, magnitude (m^2)
s_x, s_y, s_z	components of face normal vector
T	temperature (K)
t	time (sec)
$U, \tilde{U}, \hat{U}$	vectors of conserved variables
u, v, w	components of velocity (m/s)
u'	face-normal velocity (m/s)
V	element volume (m^3)
$\hat{V}$	vector of species mass fractions and vibrational energy
W	vector of source terms
X	eigenvector matrix
$\mathcal{E}$	diagonal matrix of flux correction, ϵ
ϵ	density flux correction
Λ	diagonal matrix of eigenvalues
λ_1	convective eigenvalue
ρ, ρ_s	density, species s density (kg/m^3)
τ	characteristic time (sec)
χ	diagonal elements of C
$\pm$	flux directions

I. Introduction

The solution of complex geometry nonequilibrium flows has become commonplace over the past decade. The most efficient methods use implicit time integration to solve the governing equations because of the stiffness associated with resolving cold-wall boundary layers and finite-rate chemical kinetics. Larger, more complex chemical kinetics models are beginning to be used, partly driven by the need for more accurate gas-surface interaction models. For example, recent work of Martin and Boyd[1] proposes a 38 species, 158 reaction chemical kinetics model for a pyrolyzing ablator. For some problems it may be necessary to model excited electronic states and trace species, which would further increase the computational costs beyond standard chemical kinetics models for air or other planetary atmospheres. Furthermore, recent work on vibrational state-specific models require very large numbers (potentially hundreds) of chemical species, making it impossible to apply these approaches to realistic geometries.

The computational cost of current implicit methods for aerothermodynamics problems scales quadratically with the number of equations being solved. Thus, increasing the number of chemical species drastically increases the cost of a simulation. Furthermore, these methods typically require the storage of up to seven large Jacobian matrices, which incurs large memory costs.

Popular implicit methods for aerothermodynamics solve the governing equations in a fully-coupled fashion. That is, the species mass conservation equations, momentum equations, internal energy equation(s), and total energy equation are all solved simultaneously as one large linear system of equations. For example, the data-parallel line-relaxation (DPLR) method[2] requires the solution of block tridiagonal systems of equations, where the blocks have dimension of $(ns+5)\times(ns+5)$, assuming a three-dimensional problem with a single internal energy equation, and ns is the number of chemical species. This line-relaxation approach gives excellent convergence to steady-state, but the cost of the block tridiagonal solution becomes more and more onerous as the number of species increases. The popular LAURA implicit method of Gnoffo[3] has similar quadratic cost scaling with the number of equations being solved.

In this paper, we propose a new decoupled implicit method that significantly reduces the cost of aerothermodynamics problems, while retaining the excellent convergence properties of the fully coupled line-relaxation approach. We show that the cost of this approach has nearly linear scaling with the number of species in the kinetics model. Furthermore, it requires the storage of just one large Jacobian matrix, which significantly reduces the memory requirements. With this method, the computational costs are dominated by the evaluation of the chemical source term and its Jacobian.

The concept of the proposed method is to separate the mass, momentum, and energy equations from the species mass and internal energy equations. The first set of equations is solved with the DPLR method, involving the solution of 5×5 (for three dimensions) block tridiagonal systems. Then, the implicit problem for the species mass and internal energy equations is approximated, resulting in a scalar tridiagonal system of equations to be solved. This drastically reduces the cost of the implicit system solution.

The proposed method is related to several previous approaches aimed at reducing the cost of solving problems with stiff finite-rate chemical kinetics. Bussing and Murman[4] developed an approach in which the convective fluxes were computed explicitly and the chemical source term was solved implicitly, reducing issues with stiffness. Shuen and Yoon[5] made some modifications to the Yoon and Jameson[6] lower-upper successive overrelaxation (LU-SSOR) implicit method to extend it to the simulation of chemically reacting flows. This approach results in a mostly scalar-tridiagonal system of equations to be solved, and requires the inversion of a $ns\times ns$ block matrix due to the source term Jacobian. Park and Yoon[7] developed an approach that takes advantage of elemental conservation to reduce the cost of the matrix inversion, though their approach is difficult to extend to arbitrary chemical kinetics models. Eberhardt and Imlay[8] proposed a modification to these methods to eliminate the need for the matrix inversion by replacing the full source term Jacobian with a diagonal matrix. This approach is appealing because it has a very low operation count, but it is not robust and may result in lack of elemental conservation due to large disparities in chemical time scales. Candler and Olynick[9] proposed a modification to the Eberhardt and Imlay approach using elemental conservation that improves the robustness of the method, but these approaches suffer from poor convergence on highly stretched grids due to the approximations made in the development of the LU-SSOR and later LU-SGS[10] implicit methods. Other, more recent approaches for aerothermal and reacting flow simulations use multigrid approaches and approximations to the source term Jacobian to reduce simulation costs.[11,12] In work related to the approach proposed here, Schwer *et al.*[13] developed a operator splitting approach that involves a chemical state time integration followed by a fluid dynamic time integration. An ordinary differential equation (ODE) solver is used for the first step, and a diagonalized alternating-direction implicit (ADI) method is used for the second step. Recently, Katta and Roquemore[14] developed a semi-implicit method for very large chemical kinetics models, in which a portion of the source term Jacobian is included in

the time integration. Lian, Xia, and Merkle[15] studied the integration of problems with strong source terms, and obtained improved convergence by modifying the source term evaluation and limiting the effective time step.

The present approach builds on the ideas and approaches presented in this previous work; it will be shown that the proposed method maintains the excellent convergence properties and lack of sensitivity to grid stretching of the DPLR method, while dramatically reducing the cost of the implicit solution for large chemical kinetics models. In the remainder of the paper, we provide a brief derivation of the DPLR method for the fully-coupled equations. We then derive the decoupled approach and outline the proposed solution strategy. We then apply the method to several test problems to assess its convergence properties and measure its computational costs versus the fully-coupled DPLR method.

II. Background: The Data-Parallel Line Relaxation Method

Consider a multi-species mixture of reacting gases. The inviscid conservation equations can be written as:

$$\frac{\partial U}{\partial t} + \nabla \cdot \vec{F} = W \tag{1}$$

This can be written in finite-volume form as:

$$\frac{\partial U}{\partial t} + \frac{1}{V}\sum_f \left(\vec{F}\cdot\vec{S}\right)^f = W \tag{2}$$

where the summation is over the faces of the element; V is the volume of the element and $\vec{S}$ is the outward-pointing surface normal vector, $\vec{S} = S(s_x\vec{\imath} + s_y\vec{\jmath} + s_z\vec{k})$. For convenience, define

$$F' = \vec{F}\cdot\frac{\vec{S}}{S} \tag{3}$$

The vector of conserved quantities and the surface-normal flux vector, F', are:

$$U = \begin{pmatrix} \rho_1 \\ \vdots \\ \rho_{ns} \\ \rho u \\ \rho v \\ \rho w \\ E_v \\ E \end{pmatrix}, \qquad F' = \begin{pmatrix} \rho_1 u' \\ \vdots \\ \rho_{ns} u' \\ \rho u u' + p s_x \\ \rho v u' + p s_y \\ \rho w u' + p s_z \\ E_v u' \\ (E+p)u' \end{pmatrix} \tag{4}$$

Where $u' = u s_x + v s_y + w s_z$, E_v is the vibrational energy per unit volume, and E is the total energy per unit volume. E is defined as

$$E = \sum_{s=1}^{ns} \rho_s c_{vs} T + E_v + \frac{1}{2}\rho\left(u^2+v^2+w^2\right) + \sum_{s=1}^{ns}\rho_s h_s^o \tag{5}$$

where c_{vs} is the specific heat of species s and h_s^o is its heat of formation per unit mass. The pressure is given by:

$$p = \sum_{s=1}^{ns} \rho_s \frac{\hat{R}}{M_s} T \tag{6}$$

where $\hat{R}$ is the universal gas constant and M_s is the species s molar mass.

One approach to evaluate the numerical fluxes is to use a modified form of Steger-Warming flux-vector splitting.[16] It should be noted that although we focus on this particular numerical flux function, the approach is extensible to other upwind-biased flux methods. The modified Steger-Warming flux is based on the fact that the flux vector is homogeneous in U, and therefore, we have:

$$F' = \frac{\partial F'}{\partial U} U = AU \tag{7}$$

The Jacobian matrix, A, can be diagonalized and written as:

$$A = X^{-1} \Lambda X \tag{8}$$

where Λ is the diagonal eigenvalue matrix. The modified Steger-Warming flux-vector splitting method obtains the direction of the fluxes by splitting the eigenvalue matrix into its positive and negative components, $\Lambda^{\pm}$. The split Jacobians, $A^{\pm}$, are then formed from $\Lambda^{\pm}$. Then, we can obtain an upwind-biased numerical flux across a finite-volume face using:

$$F'^f = A^{+f} U^L + A^{-f} U^R \tag{9}$$

where the L and R superscripts indicate left- and right-biased extrapolations of the conserved variables to the face. The split Jacobians are evaluated using left and right data averaged to the element face, f. Unlike the original Steger-Warming approach,[17] they are evaluated with the same data, which produces less dissipation and a more accurate flux.[16]

Now consider an implicit time integration method, in which we evaluate the fluxes and source vector at the future time level:

$$\frac{\partial U^n}{\partial t} + \frac{1}{V} \sum_f \left(F'^{n+1} S \right)^f = W^{n+1} \tag{10}$$

and then we linearize using:

$$\begin{aligned} F'^{n+1} &\simeq F'^n + \frac{\partial F'}{\partial U}^n \delta U^n \\ W^{n+1} &\simeq W^n + \frac{\partial W}{\partial U}^n \delta U^n \end{aligned} \tag{11}$$

with $\delta U^n = U^{n+1} - U^n$. Then the discrete form of the conservation equation becomes:

$$\frac{\delta U^n}{\Delta t} + \frac{1}{V} \sum_f \left(A^{+f} \delta U^L + A^{-f} \delta U^R \right)^n S^f - \frac{\partial W}{\partial U}^n \delta U^n = -\frac{1}{V} \sum_f \left(F'^n S \right)^f + W^n \tag{12}$$

This problem can be solved with a variety of methods; one approach is the data-parallel line-relaxation (DPLR) method.[2] This approach solves a line-relaxation problem along lines of elements near solid surfaces; the off-line terms on the left-hand side of the equation are updated during the relaxation process. This method involves a series of relaxation steps for δU^n and can be written as:

$$\begin{aligned} &\delta U^{(0)} = 0 \\ &\texttt{for } k = 1, k_{\max} \\ &\quad \frac{\delta U^{(k)}}{\Delta t} + \frac{1}{V} \sum_{f=\ell} \left(A^{+f} \delta U^L + A^{-f} \delta U^R \right)^{(k)} S^f - \frac{\partial W}{\partial U}^n \delta U^{(k)} = -\frac{1}{V} \sum_f \left(F'^n S \right)^f + W^n \\ &\qquad - \frac{1}{V} \sum_{f \neq \ell} \left(A^{+f} \delta U^L + A^{-f} \delta U^R \right)^{(k-1)} S^f \\ &\texttt{end} \\ &\quad \delta U^n = \delta U^{(k_{\max})} \end{aligned} \tag{13}$$

where $f = \ell$ indicates the contribution to the left-hand side of the implicit problem due to the change in the solution on the line of elements. Note that because the implicit problem solves along a line of elements, δU^L and δU^R involve each element and two of its neighbors. This results in a block tridiagonal system of equations to be solved for each line of δU. Here, $k_{\max}$ is the number of relaxation steps, which is typically taken as 4 for optimal convergence.[2]

Here we have not included the viscous fluxes, however it is straight-forward to do so. Details may be found in Wright et al.[2] The approach is to linearize the $n+1$ viscous flux, F_v^{n+1} as:

$$F_v^{n+1} = F_v^n + \delta F_v^n \simeq F_v^n + M\frac{\partial}{\partial \eta}\left(N\delta U\right) \tag{14}$$

where η is the direction normal to the face, and M and N are Jacobian matrices. This results in additional matrices added to the inviscid flux vector Jacobians in the above expression; this does not change the structure of the implicit problem to be solved.

This approach is particularly effective for high-Reynolds number flows where the near-wall boundary layer must be resolved with highly-stretched grids. It has been shown that this method can be run at large time steps and converges to the steady-state solution in a number of time steps that is essentially independent of the Reynolds number or the wall-normal grid stretching.

The line-relaxation approach is much less expensive than solving the full linear system of equations. Recent work has compared this method to a direct solve using the Generalized Method of Residuals (GMRes).[18,19] It was found that the DPLR method is less costly except for certain problems where it is difficult or impossible to construct grids with lines of grid elements in the wall-normal direction. However, because the main cost of the DPLR method are the block tridiagonal solves, the computational costs (both compute time and memory) of the DPLR method scale quadratically with the number of equations being solved. Thus, its cost can become onerous when the number of chemical species is large.

III. A Decoupled Implicit Method

Consider an extension to the DPLR method that involves splitting the conservation equations into two parts. Define $\tilde{U}$ as the vector of total mass, momentum, and energy, and $\hat{U}$ as the species mass and total vibrational energy per unit volume:

$$\tilde{U} = \begin{pmatrix} \rho \\ \rho u \\ \rho v \\ \rho w \\ E \end{pmatrix}, \qquad \hat{U} = \begin{pmatrix} \rho_1 \\ \vdots \\ \rho_{ns} \\ E_v \end{pmatrix} \tag{15}$$

with corresponding flux vectors, $\tilde{F}$ and $\hat{F}$. Now solve the governing equations in two steps. First, solve for the total variables:

$$\frac{\partial \tilde{U}}{\partial t} + \frac{1}{V}\sum_f \left(\tilde{F}'^{n+1}S\right)^f = 0 \tag{16}$$

and then

$$\frac{\partial \hat{U}}{\partial t} + \frac{1}{V}\sum_f \left(\hat{F}'^{n+1}S\right)^f = \hat{W}^{n+1} \tag{17}$$

The first phase of the solution proceeds using the standard DPLR method, with a series of block-tridiagonal solves and relaxation steps for the off-line terms, as discussed above. The $\tilde{U}$ variables are

updated to the $n+1$ time level, and the non-conserved (velocity, pressure, temperature, speed of sound, etc.) variables are updated assuming that the thermo-chemical state (species mass fractions and vibrational energy) is fixed at the n state.

The solution for the $\hat{U}$ variables is somewhat different, and can be derived starting with the discrete form of the governing equation:

$$\frac{\delta\hat{U}^n}{\Delta t} + \frac{1}{V}\sum_f \left(\hat{F}'^{n+1}S\right)^f = \hat{W}^{n+1} \tag{18}$$

We have already solved for the total mass, momentum, and energy at time level $n+1$, so we can rewrite $\delta\hat{U}^n$ as

$$\delta\hat{U}^n = \rho^{n+1}\hat{V}^{n+1} - \rho^n\hat{V}^n = \rho^{n+1}\delta\hat{V}^n + \hat{V}^n\delta\rho^n \tag{19}$$

We have defined $\hat{V} = \left(c_1, \ldots, c_{ns}, e_v\right)^T$, with $c_s = \rho_s/\rho$ the mass fraction of species s and e_v the vibrational energy per unit mass, $e_v = E_v/\rho$.

For modified Steger-Warming flux vector splitting, the flux of the $\hat{V}$ variables is proportional to the flux of total mass and the total density at the cell face. Specifically, the flux of species s mass and vibrational energy are:

$$\begin{aligned} F'^f_{\rho_s} &= \left(c_s F'_\rho\right)^f + \left(c_s^L - c_s^f\right)\rho^L\lambda_1^{+f} + \left(c_s^R - c_s^f\right)\rho^R\lambda_1^{-f} \\ F'^f_{e_v} &= \left(e_v F'_\rho\right)^f + \left(e_v^L - e_v^f\right)\rho^L\lambda_1^{+f} + \left(e_v^R - e_v^f\right)\rho^R\lambda_1^{-f} \end{aligned} \tag{20}$$

where $\lambda_1^\pm$ are the eigenvalues of the Jacobian matrices $A^\pm$ corresponding to convection. We choose to approximate $\hat{F}'^{n+1}$ with

$$\hat{F}'^{n+1} \simeq \hat{F}'^n + \left(\rho^L\lambda_1^{+f}\right)^{n+1}\delta\hat{V}^{Ln} + \left(\rho^R\lambda_1^{-f}\right)^{n+1}\delta\hat{V}^{Rn} \tag{21}$$

Now consider the linearization of the source vector, $\hat{W}$, which must be consistent with the time level of the variables, $\tilde{U}$ and $\hat{V}$. The $\tilde{U}$ variables have been updated to time level $n+1$, while the $\hat{V}$ variables remain at n. The source vector is a function of $\tilde{U}$ and $\hat{V}$ variables, and therefore may be written as

$$W^{n+1} = W(\tilde{U}^{n+1}, \hat{V}^{n+1}) \simeq W(\tilde{U}^{n+1}, \hat{V}^n) + \left.\frac{\partial W}{\partial U}\right|_{\tilde{U}} \frac{\partial U}{\partial \hat{V}}\delta\hat{V}^n \tag{22}$$

where the Jacobian matrix is computed holding the $\tilde{U}$ variables fixed at $n+1$. Let

$$C = \left.\frac{\partial W}{\partial U}\right|_{\tilde{U}} \frac{\partial U}{\partial \hat{V}} \tag{23}$$

Substituting the above expressions into the discrete conservation equation, we obtain

$$\begin{aligned} \rho^{n+1}\frac{\delta\hat{V}^n}{\Delta t} + \frac{1}{V}\sum_f \left\{\rho^L\lambda_1^{+f}\delta\hat{V}^L + \rho^R\lambda_1^{-f}\delta\hat{V}^R\right\}^{n,n+1} S^f - C^{n,n+1}\delta\hat{V}^n = \\ - \frac{1}{V}\sum_f \left(\hat{F}'^{n,n+1}S\right)^f + \hat{W}^{n,n+1} - \hat{V}^n\frac{\delta\rho^n}{\Delta t} \end{aligned} \tag{24}$$

The $n+1$ values of the $\tilde{U}$ variables and the non-conserved variables are used wherever possible in this expression. The solution of this equation yields the mass fractions and vibrational energy at time $n+1$. The

non-conserved variables are re-evaluated with the updated thermo-chemical state and the solution proceeds to the next time step.

However, there is an additional requirement on the system of equations that must be considered. We know that the mass fractions must sum to unity, and therefore the change in the mass fractions must sum to zero:

$$\sum_s c_s = 1 \qquad \sum_s \delta c_s = 0 \tag{25}$$

This is a constraint on the solution, and is effectively a result of solving one extra conservation equation. We can sum the above discrete equation for δc_s over all species to obtain:

$$\frac{\rho^{n+1}}{\Delta t}\sum_s \delta c_s^n + \frac{1}{V}\sum_f \Big\{\rho^L \lambda_1^{+f} \sum_s \delta c_s^L + \rho^R \lambda_1^{-f} \sum_s \delta c_s^R\Big\}^{n,n+1} S^f = -\frac{1}{V}\sum_f \sum_s \left(\hat{F}'^{n,n+1}_{\rho_s} S\right)^f - \frac{\delta\rho^n}{\Delta t} \tag{26}$$

Note that the sum over the source vector is zero because, by construction, it does not change the total mass. Since $\sum \delta c_s = 0$, the left-hand side to the above equation must be zero (since it is proportional to $\sum \delta c_s = 0$). Thus, to satisfy the constraint on δc_s, the right-hand side of this expression must also be zero. In the limit of an infinitely accurate discretization, the face values of c_s approach the cell-centered values, and the expression would sum exactly to zero. However in discrete form, the face values will be different and the term will not sum precisely to zero. Therefore, we can enforce the constraint by forming the quantity, ϵ, by summing over all species:

$$\epsilon = -\frac{1}{V}\sum_f \sum_s \left(\hat{F}'^{n,n+1}_{\rho_s} S\right)^f - \frac{\delta\rho^n}{\Delta t} \tag{27}$$

To impose this constraint on the system of equations, define $\mathcal{E}$ as a diagonal matrix with ϵ on the diagonal, except for the vibrational energy equation, which has a zero entry on the diagonal. We then subtract $\mathcal{E}\hat{V}$ from the right-hand side of the discrete equation to obtain:

$$\begin{aligned}\rho^{n+1}\frac{\delta\hat{V}}{\Delta t} + \frac{1}{V}\sum_f \Big\{\rho^L \lambda_1^{+f}\delta\hat{V}^L + \rho^R\lambda_1^{-f}\delta\hat{V}^R\Big\}^{n,n+1} S^f - C^{n,n+1}\delta\hat{V}^n = \\ -\frac{1}{V}\sum_f \left(\hat{F}'^{n,n+1} S\right)^f + W^{n,n+1} - \hat{V}^n\frac{\delta\rho^n}{\Delta t} - \mathcal{E}\hat{V}^n\end{aligned} \tag{28}$$

This is the final form of the implicit decoupled method for an inviscid reacting flow. Note that as the solution converges to steady-state, ϵ approaches zero because $\delta\rho$ approaches zero and the total mass flux balances at steady-state. Furthermore, when $\delta\hat{V}$ and $\delta\rho$ approach zero, the original conservation-law form of the species mass equations are obtained and therefore species mass and elements are conserved by the steady state solution. Thus, ϵ is used to maintain stability and physical consistency during convergence.

One additional point must be made concerning the consistency of the solution between the two sets of variables. It is obvious that we require that the sum of the species mass fluxes be exactly equal to the total mass flux. That is when the fluxes are evaluated with the same data, we obtain:

$$\sum_s \left(\hat{F}'_{\rho_s} S\right)^f = \left(\tilde{F}'_\rho\right)^f \tag{29}$$

However, note that the fluxes depend on the variation of the thermodynamic properties between the cell centers and faces. This variation must be included in the evaluation of $\tilde{F}'_\rho$ so that it is consistent with the

species mass fluxes. In practice, this requires forming the species mass fluxes and summing them to obtain the total mass flux. If this is not enforced, the decoupled solution will differ from the fully-coupled result.

Including the viscous fluxes in the calculation is straight-forward. For the total variables, we linearize the viscous flux using a standard approach.[3] This results in dense Jacobian matrices that are added to the implicit problem without increasing its solution cost. For the $\hat{V}$ variables, the viscous flux Jacobian matrix is almost diagonal. With Fickian diffusion (species mass diffusion proportional to the species mass fraction gradient), the only non-zero elements for the species equations are on the diagonal. For the diffusive vibrational energy transport, there is a flux due to the diffusion of each species vibrational energy. These terms result in non-zero off-diagonal entries in the viscous flux Jacobian; however, through testing we have found that they can be neglected without adversely affecting the convergence properties of the method. Thus, the addition of the viscous fluxes augments the flux vector and modifies the diagonal elements of the implicit system of equations. Therefore, it does not change the cost of solving the decoupled system.

IV. Solution of the Decoupled Implicit Problem

It is not immediately obvious that the decoupled approach will result in a large computational savings. We have apparently traded one large implicit problem for two smaller problems, potentially with limitations on the stability due to the decoupling of the two equation sets. However, we have found that it is possible to dramatically reduce the difficulty of solving for the $\hat{V}$ variables by making some additional approximations to the implicit problem.

In the final expression obtained above, note that the off-diagonal terms in the linear system of equations for $\delta\hat{V}$ are diagonal matrices of the form $\rho^f \lambda_1 I$, plus the contribution due to the linearization of the viscous fluxes. Also, the source vector Jacobian matrix is, in general, a dense matrix because any species can react with any other species. However, this matrix has a particular structure due to the form of the law of mass action. Note that the destruction of a chemical species is proportional to itself, and that its formation rate primarily depends on different chemical species. Thus, when moved to the implicit side of the equation, the source term Jacobian increases the diagonal elements and decreases the off-diagonal elements of the matrix operating on $\delta\hat{V}$. This observation is used in the work of Katta and Roquemore[14] in their semi-implicit method. The Landau-Teller expression for the vibrational energy relaxation shares this property. Therefore, we can use this property to split the source vector Jacobian into its diagonal elements and its non-diagonal elements to make a much simpler implicit problem. Let us define $\chi = \mathrm{diag}(C)$. Then, we have:

$$\begin{aligned} \rho^{n+1}\frac{\delta\hat{V}}{\Delta t} + \frac{1}{V}\sum_f \left\{\rho^L \lambda_1^{+f}\delta\hat{V}^L + \rho^R\lambda_1^{-f}\delta\hat{V}^R\right\}^{n,n+1} S^f - \chi^{n,n+1}\delta\hat{V}^{(k)} \\ = -\frac{1}{V}\sum_f \left(\hat{F}'^{n,n+1}S\right)^f + \hat{W}^{n,n+1} - \hat{V}^n\frac{\delta\rho^n}{\Delta t} - \mathcal{E}\hat{V}^n + (C-\chi)^{n,n+1}\delta\hat{V}^n \end{aligned} \tag{30}$$

For simplicity, we have not included the viscous terms in this expression. However, its form is unchanged when these terms are added. This system of equations can be solved with a modified version of the DPLR

method, given by:

$$
\begin{aligned}
&\delta\hat{V}^{(0)} = 0 \\
&\texttt{for } k = 1, k_{\max} \\
&\quad \rho^{n+1}\frac{\delta\hat{V}^{(k)}}{\Delta t} + \frac{1}{V}\sum_{f=\ell}\Big\{\rho^L\lambda_1^{+f}\delta\hat{V}^L + \rho^R\lambda_1^{-f}\delta\hat{V}^R\Big\}^{(k),n+1} S^f - \chi^{n,n+1}\delta\hat{V}^{(k)} = -\frac{1}{V}\sum_f \left(\hat{F}'^{n,n+1}S\right)^f + \hat{W}^{n,n+1} \\
&\qquad - \hat{V}^n\frac{\delta\rho^n}{\Delta t} - \mathcal{E}\hat{V}^n - \frac{1}{V}\sum_{f\neq\ell}\Big\{\rho^L\lambda_1^{+f}\delta\hat{V}^L + \rho^R\lambda_1^{-f}\delta\hat{V}^R\Big\}^{(k-1),n+1} S^f + (C-\chi)^{n,n+1}\delta\hat{V}^{(k-1)} \\
&\texttt{end} \\
&\quad \delta\hat{V}^n = \delta\hat{V}^{(k_{\max})}
\end{aligned}
\tag{31}
$$

Note that all of the terms on the left-hand side of this equation are diagonal matrices, making the line-solve a simple scalar tridiagonal problem.

V. Relative Costs of the Methods

To more clearly illustrate the savings of this approach, consider a schematic of the line-solve that must be performed by the fully-coupled DPLR method. For simplicity, let us assume that we are computing on a two-dimensional i, j structured grid. Then, for the fully-coupled problem we must solve the following expression along each constant i-line of data:

$$
\begin{pmatrix}
\ddots & \ddots & \ddots & & & & \\
 & \square & \square & \square & & & \\
 & & \square & \square & \square & & \\
 & & & \square & \square & \square & \\
 & & & & \ddots & \ddots & \ddots
\end{pmatrix}
\begin{pmatrix} \vdots \\ \delta U_{i,j-1} \\ \delta U_{i,j} \\ \delta U_{i,j+1} \\ \vdots \end{pmatrix}^{(k)}
=
\begin{pmatrix} \vdots \\ \mathrm{RHS}_{i,j} \\ \vdots \end{pmatrix}^{n}
- \square\delta U_{i+1,j}^{(k-1)} - \square\delta U_{i-1,j}^{(k-1)}
\tag{32}
$$

Here, the $\square$ represents a Jacobian matrix of dimension $ne \times ne$, where ne is the number of equations being solved. We factor the block tridiagonal system once, and then perform a backwards substitution for each relaxation step. The cost of solving this system scales quadratically with the number of equations being solved.

For the decoupled method, we solve one small system as shown above (the block matrices are 4×4 for 2-D and 5×5 for 3-D) and then we solve a problem that can be represented schematically as:

$$
\begin{pmatrix}
\ddots & \ddots & \ddots & & & & \\
 & \diagdown & \diagdown & \diagdown & & & \\
 & & \diagdown & \diagdown & \diagdown & & \\
 & & & \diagdown & \diagdown & \diagdown & \\
 & & & & \ddots & \ddots & \ddots
\end{pmatrix}
\begin{pmatrix} \vdots \\ \delta\hat{V}_{i,j-1} \\ \delta\hat{V}_{i,j} \\ \delta\hat{V}_{i,j+1} \\ \vdots \end{pmatrix}^{(k)}
=
\begin{pmatrix} \vdots \\ \hat{\mathrm{RHS}}_{i,j} \\ \vdots \end{pmatrix}^{n}
- \diagdown\delta\hat{V}_{i+1,j}^{(k-1)} - \diagdown\delta\hat{V}_{i-1,j}^{(k-1)} + \boxtimes\delta\hat{V}_{i,j}^{(k-1)}
\tag{33}
$$

Where the $\diagdown$ represents a diagonal matrix, and $\boxslash$ a square matrix with zeros on the diagonal. These matrices have dimension of $(ns+1) \times (ns+1)$. Clearly, this is a much simpler system whose solution cost is almost linear in the number of equations (the matrix-vector multiply on the right-hand side is the only quadratic operation).

The number of sub-iterations, $k_{\max}$, used in this update needs to be chosen for optimal convergence and computational cost. Since the matrix-vector multiply on the right-hand-side of (33) is the only term with quadratic scaling, limiting the number of sub-iterations may be cost-effective. We find that for cases studied here, setting $k_{\max}$ to 1 or 2 is usually optimal, and additional sub-iterations do not significantly improve the convergence rate. Thus, in the remainder of the paper we use $k_{\max} = 2$. For large numbers of chemical species, the computational cost could be reduced slightly by using a smaller value of $k_{\max}$.

Figure 1 plots the computational cost (arbitrary units of time) of the two implicit solution approaches for a two-dimensional problem as a function of the number of chemical species in the kinetics model. Here, we plot the cost of the fully-coupled implicit solve using the DPLR method versus the sum of the small block solve and the decoupled scalar tridiagonal solve. Note that the fully-coupled method scales quadratically with the number of chemical species, while the decoupled approach shows essentially linear scaling, as expected. Figure 2 plots the speedup, which is the cost of the fully-coupled implicit DPLR solve divided by the total cost of the decoupled implicit solve. The speedup is essentially linear in the number of equations, and reaches very large values for large numbers of chemical species.

For the DPLR implicit problem shown above, each grid point requires the storage of 5 block matrices for the 2-D problem (7 in 3-D). For large chemical models, this represents the largest memory cost of the method, and this requirement can limit the size of problem that may be run on a given machine. For the decoupled approach, the small DPLR problem for the total variables is relatively inexpensive, and only a single block Jacobian matrix must be stored for the species conservation equations. Thus, in the limit of large chemical models, the relative memory cost of the decoupled method will be approximately 1/5 for 2-D and 1/7 for 3-D.

VI. Test Cases

A. Blunt-Body Flows

We have implemented the proposed decoupled implicit method in a parallelized unstructured grid code[20] for three-dimensional flows; this code can also be run using the fully-coupled DPLR method. A series of test cases was run using a simple 128×128 grid on a sphere-cone geometry (10 cm nose radius, 1.1m long, 8° cone angle). The baseline free-stream conditions were taken as: $\rho_\infty = 0.001\,\mathrm{kg/m^3}$, $T_\infty = 226\,\mathrm{K}$, a Mach number of 15, and an isothermal wall of 500 K. The grid spacing at the surface was chosen so that the cell Reynolds number based on wall conditions was less than 2, which results in sufficient boundary layer resolution for accurate heat transfer rate predictions. Additional cases were run to examine the relative performance of the proposed method as the free-stream conditions are varied.

Several chemical kinetics models were used in the simulations. They range from the most basic single-species gas model with N_2 and a single vibrational energy mode to a 38 species air-carbon-hydrogen model with 49 vibrational energy modes and 158 chemical reactions. We used a 5-species air model with the species N_2, O_2, NO, N, O, and 5 reactions; the 11-species air model adds N_2^+, O_2^+, NO^+, N^+, O^+, and e^- to those species, and includes a total of 19 reactions. We also implemented a 21-species air-carbon-hydrogen model

that augments the above model with CO_2, CO, C_2, C_3, CN, H_2, HCN, C, C^+, and H; this involves a total of 32 reactions. We then added OH, CH_4, CH_3, CH_2, CH, CN^+, CO^+, H^+; this increases the number of reactions to 76. Finally, we implemented the model proposed by Martin and Boyd[1] that includes 38 species and 158 reactions. This involves adding a number of polyatomic hydrocarbons to the species listed above. The chemical rate data were taken from Park[21] and Martin and Boyd. A Landau-Teller model for the vibrational energy relaxation was used along with Millikan-White relaxation times. This is the standard vibrational energy relaxation model used for re-entry flow simulations. Most cases were run with a non-catalytic boundary condition; it was found that a fully-catalytic boundary condition does not adversely affect the convergence properties of the method.

The flow field was initialized as free-stream and integrated to steady-state conditions. The initial phase of the simulations is violent, with a strong shock wave forming near the surface and moving away from the surface until it reaches its equilibrium condition. During this process, both methods require that the time step be started at a small value and then gradually increased as the bow shock wave begins to approach its equilibrium position. It is difficult to determine the optimal time-step ramping schedule; in each case, we experimented with increasingly aggressive time steps until the run would complete and steady-state convergence was obtained. In general, the decoupled method could be run with similar or the same time steps as the fully-coupled method, though in some cases, the maximum time step of one or the other method was more limited. However, as we will see, this limitation does not significantly affect the convergence history.

Both methods have been shown to converge to machine zero; now the question is whether they produce the same result on a given grid. For this blunt-body test case, we consider the surface heat flux and stagnation-line chemical state as sensitive measures for evaluation of the new method. These quantities are plotted in Figs. 3 and 4. Note that as plotted, the results of the two methods over-plot one another for this test case. More quantitatively, the stagnation point heat flux predicted by the two methods are within 0.1% of one another. The stagnation point heat flux is notoriously difficult to compute and small differences in numerical dissipation can change the results.[22] The chemical mass fractions are identical to 4 digits of accuracy. Thus, for this case, the decoupled method produces essentially identical results as the DPLR method. Below, we will see that for a more challenging problem the differences are larger, but systematically converge as the grid is refined.

Convergence to steady-state was monitored with the L_2 norm of the density residual, defined as:

$$L_2^n = \frac{1}{\Delta t}\sqrt{\sum_{i,j}\left(\Delta\rho_{i,j}^n\right)^2} \tag{34}$$

Where $\Delta\rho^n$ is computed in each finite volume from the net mass flux balance at each time step:

$$\Delta\rho_{i,j}^n = \frac{1}{V}\sum_f \left(F_\rho'^n S\right)^f \tag{35}$$

Thus, this is a direct measure of the balance of the mass fluxes into and out of each grid element. When the density residual approaches machine zero, the solution is converged. For plotting purposes, we normalize by the initial L_2 norm.

Figure 5 plots the convergence history for the Mach 15 test case computed using the 21-species, 32-reaction chemical kinetics model. We use a free-stream composition that is 90% air and 10% CO_2 by mass.

Note that the two methods converge to steady-state in about 800 time steps. For this case, the decoupled method is 4.2 times faster than the fully-coupled DPLR method, and therefore it converges to steady state in about 240 seconds, compared to 1000 seconds for the fully-coupled code. (These simulations were run on 3.2 GHz Intel Nehalem workstation.) The maximum time step was the same for both methods, corresponding to a CFL number of 5000. The CFL number is defined as the time step divided by the characteristic time scale, τ, which is given by

$$\tau = \min_{i,j} \frac{\Delta}{|\vec{u}| + a} \tag{36}$$

where Δ is the minimum dimension of the grid element, and a is the local speed of sound. In this case, the maximum time step corresponds to about $10\,\mu$sec.

Additional cases were run to assess the performance of the decoupled method for more challenging conditions. Figure 6 plots the convergence history for two cases: a Mach 20 flow at the same free-stream conditions as discussed above, but with an isothermal wall set to $T_w = 1000\,\mathrm{K}$; and a Mach 25 flow with a free-stream density of $10^{-4}\,\mathrm{kg/m^3}$ and $T_w = 1500\,\mathrm{K}$. For both cases the 11-species, 19-reaction air model was used. Note that the Mach 20 case takes approximately twice as many time steps to converge, and that the decoupled method requires about 100 additional time steps to reach machine zero. However, it is 3.4 times faster than the fully-coupled DPLR method, resulting in a significant reduction in run time. Interestingly, for the Mach 25 case, the decoupled method converges slightly faster than the fully-coupled method.

From these results, we see that the proposed decoupled method converges in approximately the same number of time steps as the fully-coupled DPLR method. Additional cases have been run with catalytic walls, a range of wall temperatures, at larger densities, and to date this observation holds for all cases studied. As discussed above, the cost of the decoupled implicit solution is significantly reduced, resulting in substantially reduced run times with the new method. Figure 7 quantifies the overall speedup of the decoupled method as a function of the number of chemical species in the chemical kinetics model. Note that as expected the decoupled method is substantially faster and the speedup increases with the number of equations being solved. However, the speedup is not as large as shown in Figure 2. This is because we are now considering the relative speedup of the entire code, rather than just the implicit solve.

Figure 8 plots the cost of running 100 time steps of each part of the solution for the two methods as a function of the number of chemical species in the model – note the different scales on the time axis. We see that for the original DPLR method, the cost of evaluating the fluxes and the associated Jacobian matrices scales approximately linearly with the number of species, while the other two components scale quadratically. The cost of evaluating the chemical source term and its Jacobian remains a fairly small fraction of the total cost, even with a 38-species model. Thus, the cost for the DPLR method is mostly driven by the solution of the implicit block tridiagonal problem.

With the decoupled method, the implicit solution scales nearly linearly and its cost becomes only a small fraction of the total cost as the number of chemical species gets large. With this method, the cost of evaluating the chemical source term dominates the overall solution cost. This is to be expected because as the number of chemical species increases, the number of possible reactions increases quadratically because any species can react with any other species. For example, the 11-species model has 19 reactions, the 21-species model has 32 reactions, the 29-species model has 76 reactions, and the 38-species model has 158 reactions. Clearly, the cost of evaluating the chemical source term increases significantly. This is a variant of Amdahl's law: in the limit, the solution can only be as fast as its slowest part. However, even with this

expensive source term evaluation, the new method is 4.6 times faster for the 38-species case. This speedup would increase for larger chemical kinetics models.

B. Double-Cone Flows

Now let us consider a different test case to explore how the proposed decoupled method performs on a more challenging flow field. The hypersonic double-cone flow has been the subject of several code validation studies.[23,24] The geometry of this problem is simple: a 25° half-angle cone joined to a 55° half-angle cone; both of which have the same surface length. The first cone produces an attached shock wave, while the second cone produces a detached bow shock. The flow separates due to the change in cone angle, which produces a separation shock. These non-linear process are tightly coupled to one another, and amplify small errors in numerical or physical modeling. This sensitivity affects the surface properties (particularly heat flux), making it possible to make direct comparisons to experimental data.[25,26] The relative spatial accuracy of a given numerical method can be inferred from the variation of the separation zone size with grid resolution; in general, more accurate methods produce larger separation zones.[27]

The conditions chosen here are particularly challenging, corresponding to a high-enthalpy test in the CUBRC Inc. LENS-I reflected shock tunnel facility.[24] The flow conditions are air at: $\rho_\infty = 2.0 \times 10^{-3}\,\mathrm{kg/m^3}$, $T_\infty = 570\,\mathrm{K}$, $T_v = 720\,\mathrm{K}$, $u_\infty = 4235\,\mathrm{m/s}$, and $M_\infty = 8.83$. We use a 5-species model for air with 3 dissociation reactions and the two Zeldovich reactions involving NO. The free-stream conditions produce significant levels of O_2 dissociation in the separation region and downstream of the strong bow shock and shock triple point. Cases were run with three grids of increasing resolution: 256×128 (axial $\times$ normal), 512×256 and 1024×512. Previous work has shown that second-order accurate methods should produce converged solutions on the finest of these grids.[12,27]

Figure 9 shows the convergence histories for the two methods on each grid. For these cases, the maximum allowable CFL is capped at about 2000; attempts to run at larger time steps result in instabilities downstream of the shock interaction. Thus, the number of time steps required for convergence to steady state increases as the grid is refined. The DPLR method does not demonstrate machine-zero convergence, with a limit cycle developing just downstream of the shock triple point. The decoupled method converges to machine zero after a large number of time steps. It should be noted that this flow takes a large time to reach steady-state because of the tight coupling between the separation zone size, the separation shock, the shock interactions, and the impingement of the transmitted shock on the second cone surface.

Comparisons of flow field shows that there are small differences between the two methods near the shock triple point. In particular, on the coarse grid DPLR predicts the bow shock to be further upstream than the decoupled method. However, as the grid is refined the differences decrease so that on the fine (1024×512) grid the contour lines are essentially identical. On a more quantitative level, consider Figure 10 which plots the heat transfer rate along the surface near the separation zone and the shock impingement location. Results from the three grids are plotted, and it is apparent that the coarse grid calculations are not grid converged and barely capture the large under-shoot and over-shoot of heat flux due to the shock-boundary layer interaction. The two methods produce essentially identical results on the fine grid. Thus, as the solution becomes grid-converged the two methods produce the same results.

C. Hydrogen-Air Combustion

Finally, the flow of a stoichiometric mixture of hydrogen and air in a two-dimensional duct with a 10° ramp was considered. The duct is 3 cm long and 2 cm high, with the ramp starting 1 cm from the lower wall leading edge. The incoming flow has a temperature of 1200 K, a Mach number of 4, and a pressure of 1 atm; an adiabatic wall boundary condition is used. The boundary layer and the shock produced by the ramp cause the temperature to rise above the ignition temperature. This test case has been used by a number of researchers; see Ref. 5 for more details. The current grid is 140×200, as compared to the 90×60 grid used in previous studies.

Two H_2-air kinetics models were used: the 7-species, 8-reaction model of Evans and Schexnayder[28] and the 13-species, 33-reaction model of Jachimowski.[29] Figure 11 plots the convergence history for the DPLR and decoupled method runs. Both methods converge about 8 orders of magnitude in 600 time steps, and the convergence histories are similar to one another. There are minor differences between the convergence histories depending on the kinetics model used. For this case, the largest CFL number used was 50 for both methods (corresponding to a time step of 0.076 μsec). Larger time steps (up to CFL = 1000) result in slower convergence and limit cycles at larger values of the residual. Integrating the Evans and Schexnayder kinetics model at the adiabatic wall conditions for this test case, we find that the initial formation of water takes place in less than 1 μsec and the characteristic time scale is approximately 0.014 μsec. Thus, the CFL number used here is approximately 5 times larger than the characteristic chemical reaction time.

VII. Conclusions

Present implicit numerical methods for the simulation of aerothermodynamics and high-temperature reacting flows solve the governing equations in a fully coupled fashion. That is, they simultaneously solve the conservation equations for each chemical species mass, total momentum, internal energy (or energies), and total energy. The cost of solving the resulting system of equations scales quadratically with the number of equations. We explore a different approach, in which the total mass, momentum, and energy equations are decoupled from the species mass and internal energy conservation equations. Then the two sets of equations are solved in two steps: first the data-parallel line-relaxation (DPLR) method is used to solve the total conservation equations; then a simplified form of DPLR is used to solve the remaining equations. In particular, the off-diagonal elements of the source vector Jacobian matrix are lagged in the relaxation process, making the problem a scalar tridiagonal system. This results in a significant decrease in solution cost, both in terms of computational time and memory. We have run numerous test cases and found that the proposed decoupled method converges in essentially the same number of time steps as the fully-coupled DPLR approach. Therefore, the proposed method reduces the computational time and memory requirements by a significant margin. For the cases considered here, the decoupled method is shown to be significantly faster than the DPLR method. For example, with a 38-species 158-reaction chemical kinetics model, it is 4.6 times faster, and most of the solution time is associated with the evaluation of the chemical source term and its Jacobian matrix. For this case, the proposed method reduces the memory requirements by a factor of 4.4. The decoupled approach could be adapted to other implicit methods for high-temperature reacting flows.

Acknowledgments

This work was sponsored by the Air Force Research Laboratory under grant FA9453-12-1-0133, the Air Force Office of Scientific Research under grant FA9550-10-1-0563, and by the Department of Defense National Security Science & Engineering Faculty Fellowship. The views and conclusions contained herein are those

of the author and should not be interpreted as necessarily representing the official policies or endorsements, either expressed or implied, of the sponsors or the U.S. Government.

References

[1]Martin, A., and I.D. Boyd, "CFD Implementation of a Novel Carbon-Phenolic-in-Air Chemistry Model for Atmospheric Re-Entry," AIAA 2011-0143, Jan. 2011.

[2]Wright, M.J., D. Bose, and G.V. Candler, "A Data-Parallel Line Relaxation Method for the Navier-Stokes Equations," *AIAA Journal,* Vol. 36, No. 9, pp. 1603-1609, Sept. 1998.

[3]Gnoffo, P.A., "An Upwind-Biased, Point Implicit Relaxation Algorithm for Viscous, Compressible Perfect-Gas Flows," NASA TP-2953, 1990.

[4]Bussing, T.R.A., and E.M. Murman, "A Finite Volume Method for the Calculation of Compressible Chemically Reacting Flows," AIAA 1985-0331, Jan. 1985.

[5]Shuen, J.S., and S. Yoon, "Numerical Study of Chemically Reacting Flows Using a Lower-Upper Successive Overrelaxation Scheme," *AIAA Journal,* Vol. 27, No. 12, pp. 1752-1760, Dec. 1989.

[6] Yoon, S., and A. Jameson, "An LU-SSOR Scheme for the Euler and Navier-Stokes Equations,", AIAA 1987-0600, Jan. 1988.

[7]Park, C., and S. Yoon, "A Fully-Coupled Implicit Method for Thermo-Chemical Nonequilibrium Air at Sub-Orbital Speeds," AIAA 1989-1974, June 1989.

[8]Eberhardt, S., and S. Imlay, "A Diagonal Implicit Scheme for Computing Flows with Finite-Rate Chemistry," AIAA 1990-1577, June 1990.

[9]Candler, G.V., and D.R. Olynick, "Hypersonic Flow Simulations Using a Diagonal Implicit Method," in *Computing Methods in Applied Sciences and Engineering,* Ed. R. Glowinski, Nova Science Publishers, New York, pp. 29-47, 1991.

[10]Yoon, S., and A. Jameson, "Lower-Upper Symmetric Gauss-Seidel Method for the Euler and Navier-Stokes Equations,", *AIAA Journal,* Vol. 26, No. 9, pp. 1025-1026, Sept. 1988.

[11]Edwards, J.R., "An Implicit Multigrid Algorithm for Computing Hypersonic, Chemically Reacting Viscous Flows," *Journal of Computational Physics,* Vol. 123, pp. 84-95, 1996.

[12]Gerlinger, P., P. Stoll, and D. Brüggemann, "An Implicit Multigrid Method for the Simulation of Chemically Reacting Flows," *Journal of Computational Physics,* Vol. 146, pp. 322-345, 1998.

[13]Schwer, D.A., P. Liu, W.H. Green, and V. Semiao, "A Consistent-Splitting Approach to Stiff Steady-State Reacting Flows with Adaptive Chemistry," *Combustion Theory and Modeling,* Vol. 7, pp. 383-399, 2003.

[14]Katta, V.R., and W.M. Roquemore, "Calculation of Multidimensional Flames Using Large Chemical Kinetics," *AIAA Journal,* Vol. 46, No. 7, pp. 1640-1650, July 2008.

[15]Lian, C., G. Xia, and C.L. Merkle, "Impact of Source Terms on Reliability of CFD Algorithms," *Computers and Fluids*, Vol. 39, pp. 1909-1922, 2010.

[16]MacCormack, R.W. and G.V. Candler, "The Solution of the Navier-Stokes Equations Using Gauss-Seidel Line Relaxation," *Computers and Fluids*, Vol. 17, No. 1, pp. 135-150, 1989.

[17]Steger, J. and R.W. Warming, "Flux Vector Splitting of the Inviscid Gasdynamics Equations with Appli-

cation to Finite Difference Methods," *NASA TM-78605*, 1979.

[18]Nompelis, I., T. Wan and G. Candler, "Performance Comparisons of Parallel Implicit Solvers for Hypersonic Flow Computations on Unstructured Meshes," *AIAA-2007-4334,* June 2007.

[19]MacLean, M., and T. White, "Implementation of Generalized Minimum Residual Krylov Subspace Method for Chemically Reacting Flows," AIAA 2012-0441, Jan. 2012.

[20]Nompelis, I., T. Drayna and G.V. Candler, "A Parallel Unstructured Implicit Solver for Hypersonic Reacting Flow Simulation," *AIAA 2005-4867,* June 2005.

[21]Park, C., "Review of Chemical-Kinetic Problems of Future NASA Missions I - Earth Entries," *Journal of Thermophysics and Heat Transfer,* Vol. 7, No. 3 pp. 385-398, 1993.

[22]MacCormack, R.W., "The Carbuncle CFD Problem," AIAA-2011-0381, Jan. 2011.

[23]Harvey, J., M.S. Holden, and G.V. Candler, "Validation of DSMC/Navier-Stokes Computations for Laminar Shock Wave/Boundary Layer Interactions Part 3," AIAA-2003-3643, June 2003.

[24]Knight, D.D, J. Longo, D. Drikakis, D. Gaitonde, A. Lani, I. Nompelis, B. Reimann, L. Walpot "Assessment of CFD capability for prediction of hypersonic shock interactions," *Progress in Aerospace Sciences* Vol. 48, pp. 8-26, Jan.Feb. 2012.

[25]Nompelis, I., G.V. Candler, and M.S. Holden, "Effect of Vibrational Nonequilibrium on Hypersonic Double-Cone Experiments," *AIAA Journal,* Vol. 41, No. 11, pp. 2162-2169, Nov. 2003.

[26]Gaitonde, D.V., P.W. Canupp, M.S. Holden, "Heat Transfer Predictions in a Laminar Hypersonic Viscous/Inviscid Interaction," *Journal of Thermophysics and Heat Transfer,* Vol. 16, No. 4, pp. 481-489, 2002.

[27]Druguet, M.C., G.V. Candler, and I. Nompelis, "Effects of Numerics on Navier-Stokes Computations of Hypersonic Double-Cone Flows," *AIAA Journal*, Vol. 43, No. 3, pp. 616-623, March 2005.

[28]Evans, J.S., and C.J. Schexnayder, "Influence of Chemical Kinetics and Unmixedness on Burning in Supersonic Hydrogen Flames," *AIAA Journal,* Vol. 18, No. 2, pp. 188-193, Feb. 1980.

[29]Jachimowski, C.J., "An Analysis of Combustion Studies in Shock Expansion Tunnels and Reflected Shock Tunnels," NASA TP-3224, July, 1992.

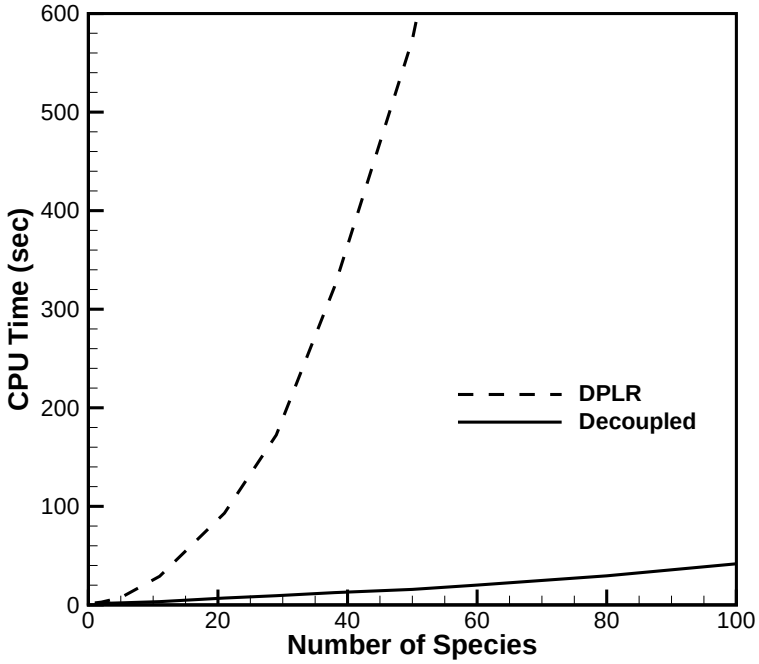

Figure 1. Computational cost of the fully-coupled data-parallel line relaxation (DPLR) implicit solve and the decoupled implicit solve for a two-dimensional problem.

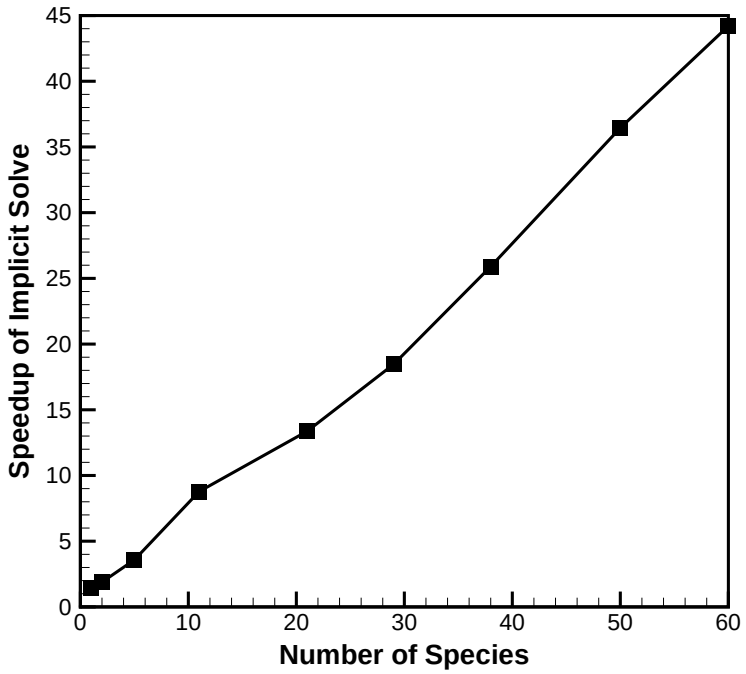

Figure 2. Speedup of the decoupled implicit solution method relative to the DPLR method as a function of the number of chemical species in the model.

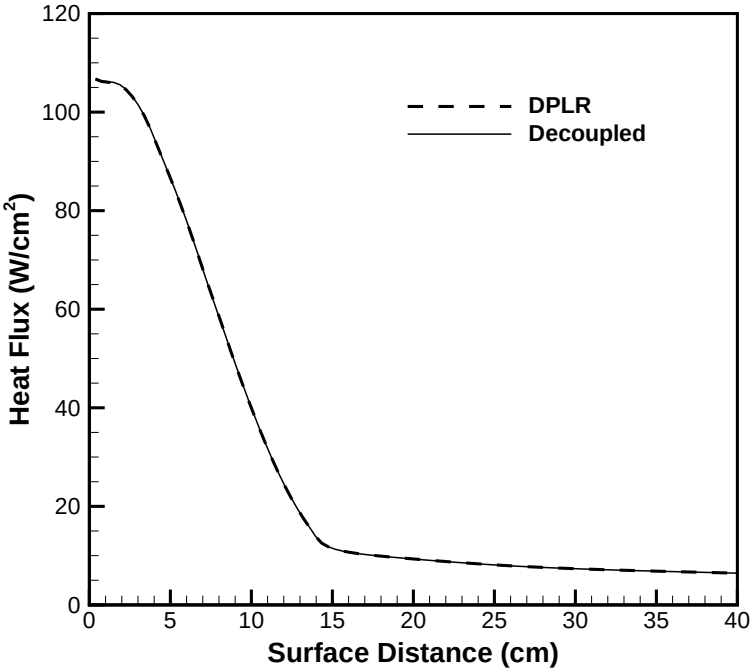

Figure 3. Computed convective heat flux for the Mach 15 test case as a function of surface distance for the DPLR and decoupled methods.

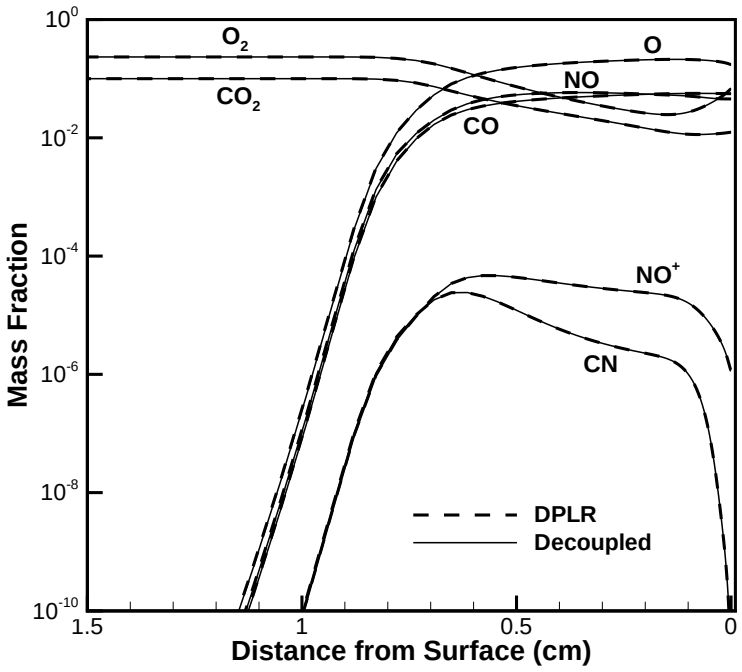

Figure 4. Computed mass fractions of selected species on the stagnation streamline for the Mach 15 test case.

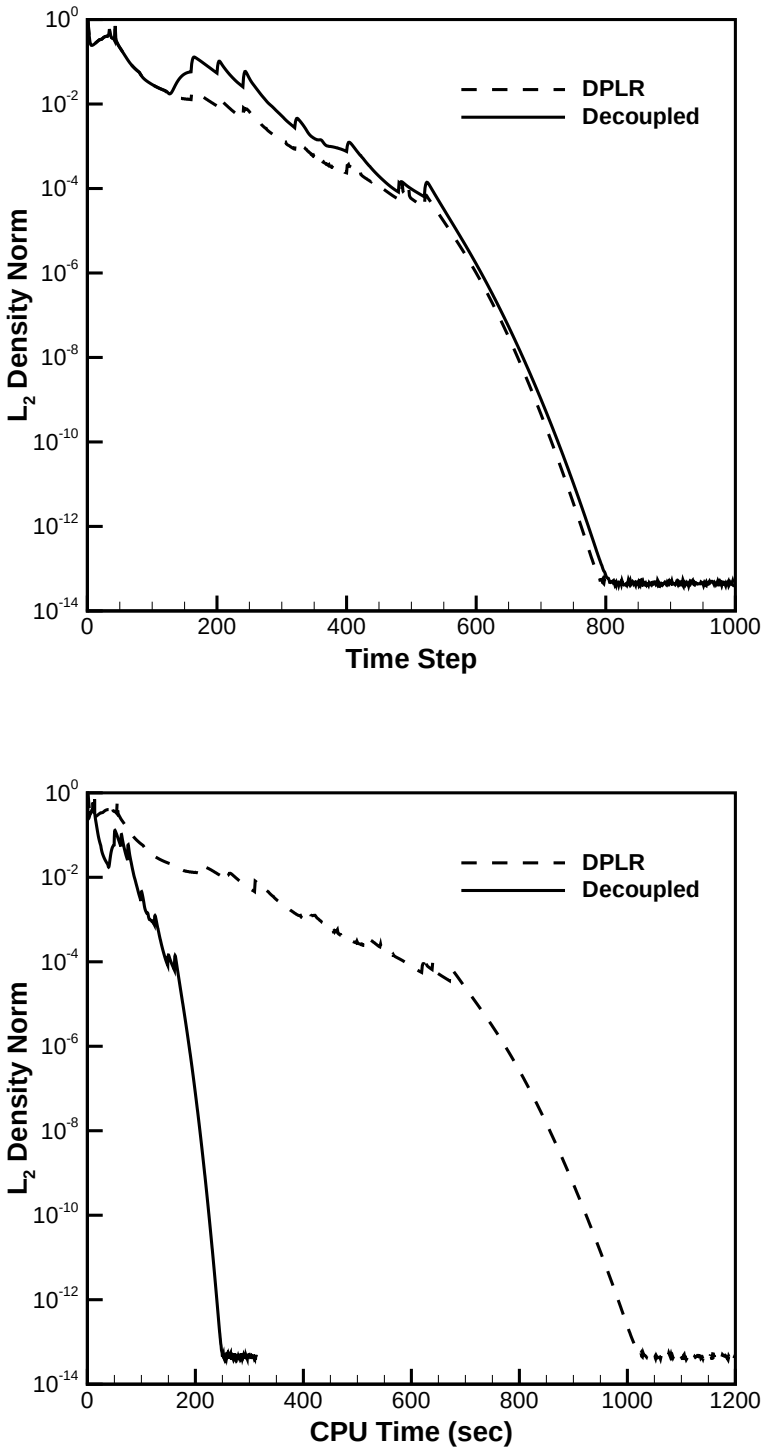

Figure 5. Convergence history and computational time for the sphere-cone test case at $M = 15$ conditions for a 21 species, 32 reaction air-CO_2 chemical kinetics model.

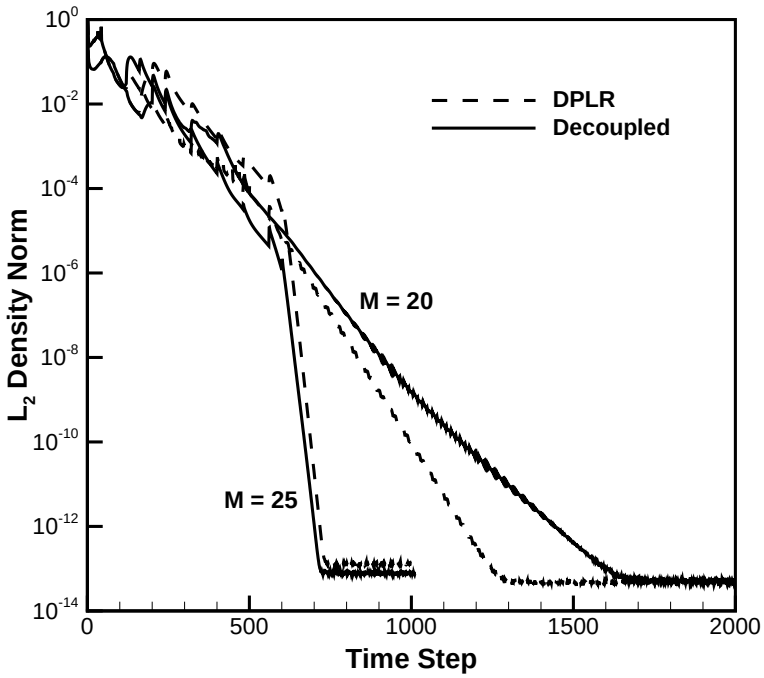

Figure 6. Convergence history for the sphere-cone test case at $M = 20$ and $M = 25$ conditions for a 11 species, 17 reaction air chemical kinetics model.

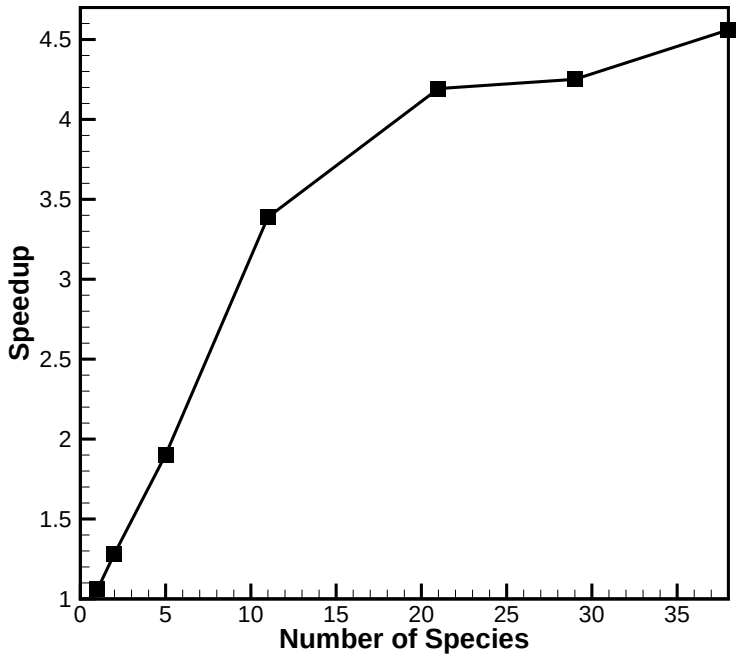

Figure 7. Speed up (ratio of DPLR to decoupled solution time) with number of chemical species.

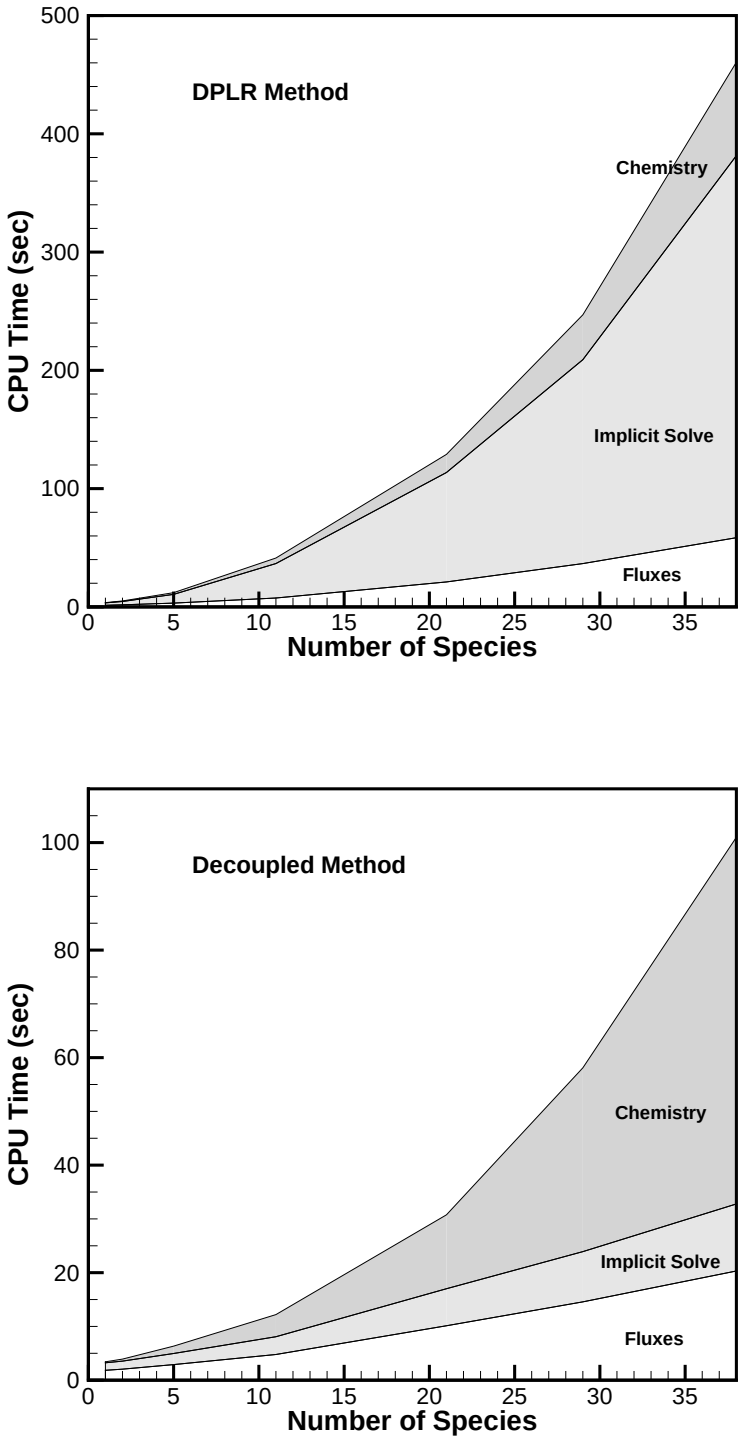

Figure 8. Cost of each part of the solution as a function of the number of chemical species: DPLR (upper); Decoupled method (lower).

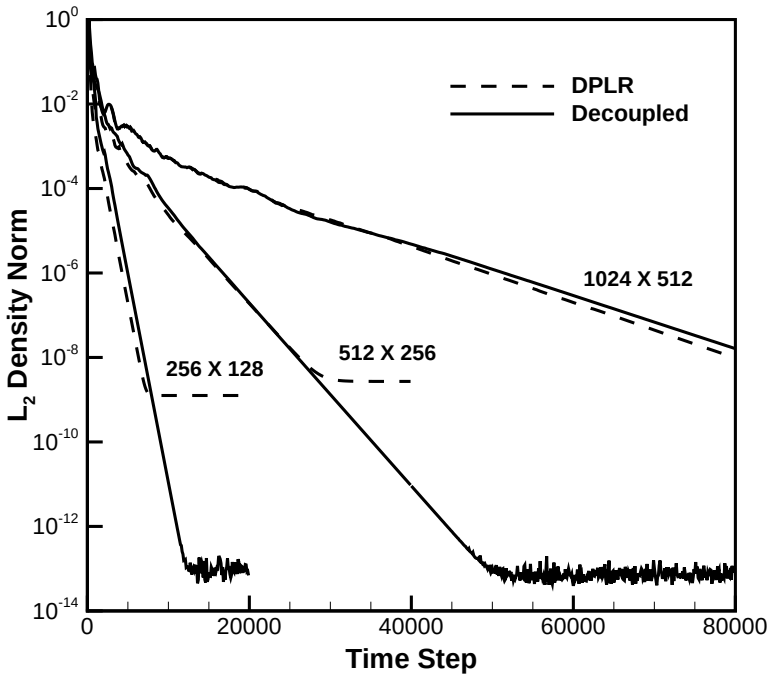

Figure 9. Convergence history for the double-cone test case.

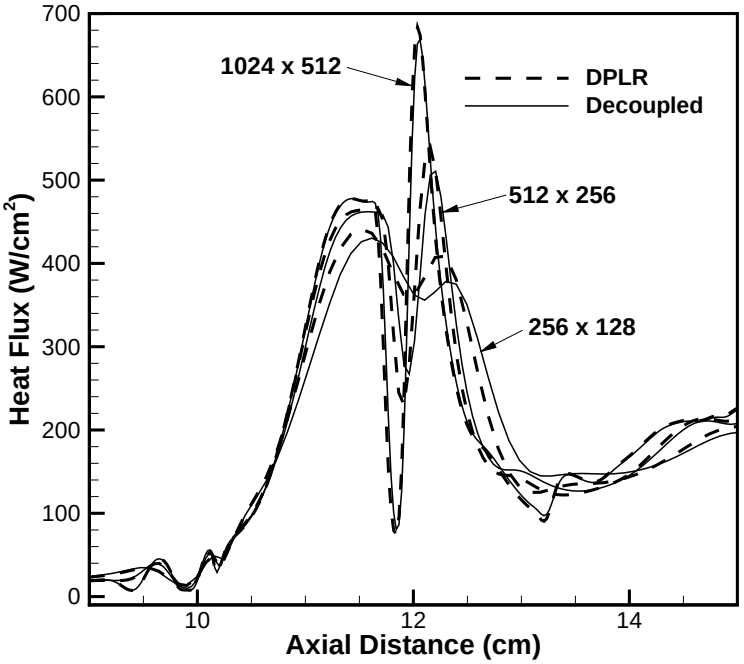

Figure 10. Computed convective heat flux for the double-cone test case in the region of the separation zone and shock impingement.

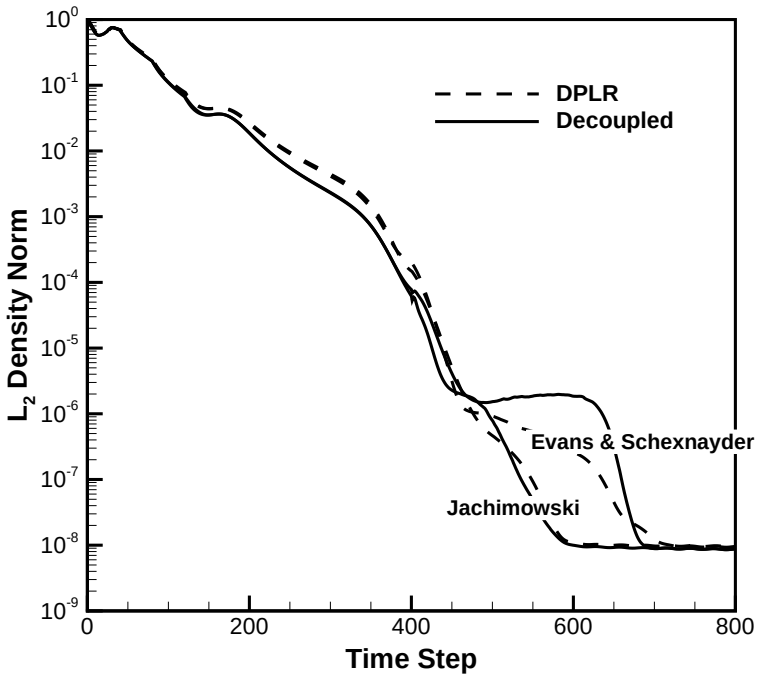

Figure 11. Convergence history for the H_2-air test case.

DISTRIBUTION LIST

DTIC/OCP
8725 John J. Kingman Rd, Suite 0944
Ft Belvoir, VA 22060-6218 1 cy

AFRL/RVIL
Kirtland AFB, NM 87117-5776 2 cys

Official Record Copy
AFRL/RVBYE/Dr. Raymond Bemish 1 cy